

# Strong Pinning and Plastic Deformations of the Vortex Lattice

A. Schönenberger<sup>a</sup>, A. Larkin<sup>b,c</sup>, E. Heeb<sup>a</sup>, V. Geshkenbein<sup>a,b</sup>, G. Blatter<sup>a</sup>

<sup>a</sup> *Theoretische Physik, ETH Hönggerberg, CH-8093 Zürich, Switzerland*

<sup>b</sup> *L. D. Landau Institute for Theoretical Physics, 117940 Moscow, Russia*

<sup>c</sup> *School of Physics and Astronomy, University Minnesota, Minneapolis, MN 55455, USA*

(October 27, 2018)

We investigate numerically the dynamically generated plastic deformations of a 3D vortex lattice (VL) driven through a disorder potential with isolated, strong pinning centers (point-like or extended along the field direction). We find that the VL exhibits a very peculiar dynamical behavior in the plastic flow regime, in particular, topological excitations consisting of three or four entangled vortices are formed. We determine the critical current density  $j_c$  and the activation energy for depinning  $U_c$  in the presence of a finite density of strong pinning centers.

PACS numbers: 74.60.-w, 74.60.Ge

Recently, the dynamical behavior of a VL in a disordered type-II superconductor has attracted much interest [1–3]. The intriguing dynamics of the VL originates from the competition between the vortex – defect and the vortex – vortex interaction, leading to a threshold behavior [4]: If the pinning potential dominates then the vortices are essentially stationary with a slow residual motion due to tunneling or thermal activation. In the opposite limit, when the pinning forces are weak compared with the driving force, the VL is only elastically deformed and flows coherently. In the important intermediate regime, when the pinning and driving force are comparable, the VL deforms plastically and an incoherent motion results [5,6]. The breakdown of the weak collective pinning scenario [7] with increasing strength of the pinning potential has been observed in numerical simulations [8]. Furthermore, it has numerically been shown [8,9] that the plastic flow of a 2D VL driven through a random pinning potential consists of channels of flowing vortices, i.e., *rivers*, and regions of pinned vortex lines, i.e., *islands*. This so-called channel flow behavior has been observed experimentally by means of Lorentz microscopy [10,11]. The various anomalies [3,12] (e.g., thermal instability at large currents, non-monotonicity of the  $I$ - $V$  curves, peak effect) occurring in the plastic flow regime suggest that the nature of the dynamics is fundamentally dissimilar from the one in the elastic regime. In particular, the dynamically generated disorder is of general importance as it seems to be a basic constituent of the dynamics in disordered systems.

In this paper we present for the first time a study on the dynamically produced defects in a 3D VL. We concentrate on a VL driven through a material with isolated strong pinning centers. It turns out that such strong pinning centers can entail the generation of localized topological excitations involving three or four entangled vortices. Moreover, the presence of strong pins leads to a preferred orientation of motion of the VL and affects the critical current density as well as the barrier for depinning. In the following we first introduce our model and then consider point-like as well as extended pinning centers.

If the density of *defects* is low, the VL deformations produced by individual pinning centers can be studied without accounting for collective effects. The pinning centers con-

sidered here are assumed to have a rod-like shape with a small lateral (coherence length  $\sim \xi$ ) but a variable longitudinal (from  $\xi$  to a few lattice constants  $a_0$  along the field direction) extension. This kind of defects corresponds, for instance, to the discontinuous columns of damaged material, e.g.,  $\text{YBa}_2\text{Cu}_3\text{O}_7$  irradiated with 0.58 GeV Sn ions [13], to carbon nanotubes embedded in  $\text{Bi}_2\text{Sr}_2\text{CaCu}_2\text{O}_x$  [14] or to MgO nanorods grown in BSCCO superconductors [15]. The pinning force with a range of the order of  $\xi$  is taken to be infinitely large – a trapped vortex segment cannot escape from the pinning center – and, therefore, only the interaction between the vortices is relevant. This assumption is physically reasonable since the maximal force the vortices exert on the pinned vortex segment is much smaller than the maximal possible force resulting from the depairing current. The driving force acting on the vortices is in the plane perpendicular to the VL and the magnetic field is restricted to  $B < 0.2H_{c2}$ , i.e., the London approximation can be used, and to  $\lambda > a_0 = \sqrt{\Phi_0/B}$ , where  $\lambda$  is the London penetration depth. These restrictions on the magnetic field are not severe as most of the experimentally accessible regime is covered. Within this regime, the scaling rules [16] are applicable allowing to generalize the results obtained for isotropic superconductors considered in the following. For convenience and technical reasons the moving VL is chosen as the frame of reference and hence the pinning center appears to move through the VL. In order to describe the lattice deformation produced by a defect we allow a finite number of *soft* vortices in the neighborhood of the pinned vortex line to accommodate according to their interaction. All other vortices are held fixed and consequently denoted as *hard* vortices. Accordingly, we split the (isotropic) London energy functional for the soft vortices

$$F = \frac{\varepsilon_0}{2} \sum_{i,j} \int d\mathbf{r}_i \cdot d\mathbf{r}_j \frac{e^{-\sqrt{|\mathbf{r}_i - \mathbf{r}_j|}/\lambda}}{\sqrt{|\mathbf{r}_i - \mathbf{r}_j|}}, \quad (1)$$

into three different parts: The self interaction accounting for the line energy of the soft vortices, the mutual interaction of the soft vortices, and the coupling of the soft vortices to the surrounding hard vortices. The instability to fluctuations of the energy functional (1) is cured by taking a core term into account and by using a cutoff  $\sim \xi$ . The algorithm to relax the vortices is based on a conjugate gradient method; for details on the numerics,

see Ref. [17]. We do not investigate the mechanism of vortex trapping and, therefore, the pinning center considered is initially positioned at a lattice site. The pinning center fixes the vortex along its length  $l_p$ . Subsequently, the pinning center together with the attached vortex segment is adiabatically dragged through the VL while the deformation energy of the VL is monitored. The parameters in this procedure are the dragging angle  $\vartheta$  with respect to a basis lattice vector, the distance  $d$  from the equilibrium lattice site, and the length  $l_p$  of the pinning center. The energy per length of the lattice deformations is measured in units of  $\varepsilon_0$ , where  $\varepsilon_0 = (\Phi_0/4\pi\lambda)^2$ , and the lattice spacing  $a_0$  is used as the length unit.

The *point-like pinning centers* have an extension of  $3\xi$  along the field direction and the magnetic field  $B \approx 0.0025H_{c2}$  is fixed by setting  $a_0/\xi = 50$ . Note that the pinning length  $l_p = 3\xi$  is larger than the cutoff  $\xi$  of the energy functional but still small enough to correspond to point-like pins. Quantitatively similar results are obtained when  $l_p$  is doubled. Estimates on elastic deformations of the VL suggest that the set of soft vortices should include the pinned vortex as well as the nearest neighboring vortices. Small displacements of the pinned vortex segment entail pronounced deformations only close to the pin where sharp kinks occur. With increasing displacement  $d$  the parts of the pinned vortex above and below the pin tend to align anti-parallel and, therefore, attract each other, see Fig. 1. At the critical distance,  $d_{dp} = 0.22a_0$ , this attraction dominates and makes the configuration collapse, i.e., the two anti-parallel vortex segments annihilate, leaving behind a free unpinned vortex and a vortex loop attached to the pin. Subsequently, the free vortex line relaxes to its equilibrium lattice position and the vortex loop shrinks and disappears. With this *one-loop depinning* process the pin is freed and hence the VL becomes unpinned. Note that the change in topology is mediated by vortex cutting and recombination. The deformation energy versus the displacement is shown in Fig. 1. The sharp edge of the deformation energy at the recombination of the vortices, see Fig. 1, strongly influences the exponent in the scaling law of the depinning barrier and, in particular, seems to be the signature of depinning from strong pins. As the depinning distance  $d_{dp} = 0.22a_0$  is rather small, the pinned vortex line does neither noticeably affect the other vortices during the dragging process nor experience

the non-circularity of the hexagonal VL potential. Consequently, the whole dragging process is essentially circular symmetric rendering the energy of the lattice deformation as well as the depinning mechanism independent of the angle. As a result, the presence of point-like pinning centers does not ensue a preferred orientation for a moving VL and, in addition, no vortex entanglement is introduced.

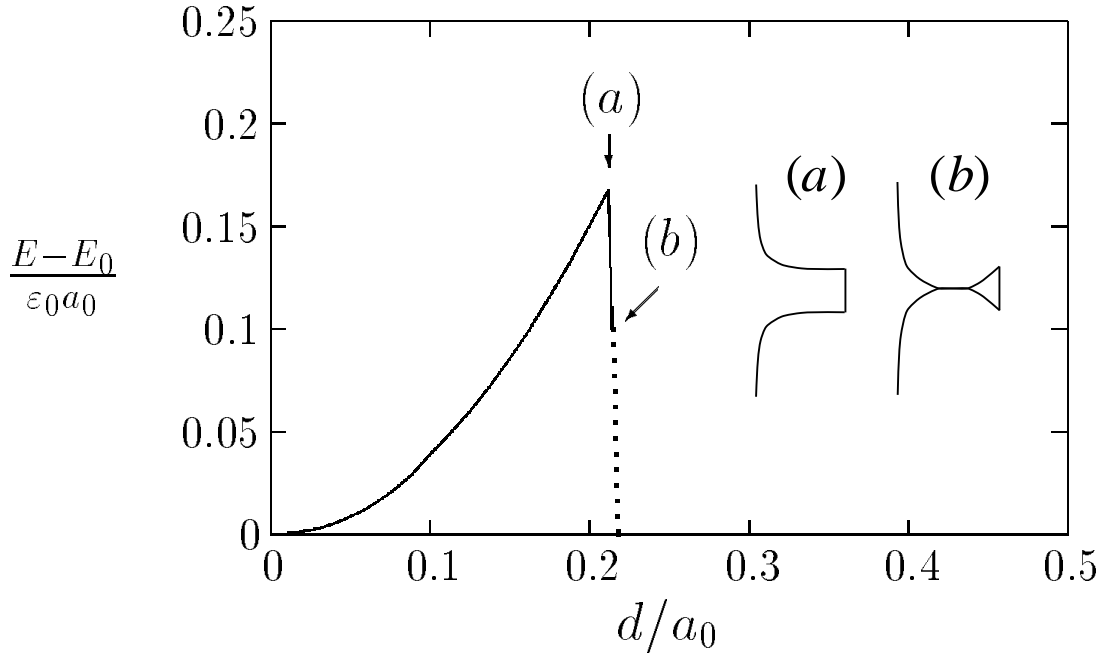


FIG. 1. The deformation energy as a function of the displacement of the pinned vortex segment is independent of the angle  $\vartheta$  (the curves  $\vartheta = 0^\circ$ ,  $15^\circ$ , and  $30^\circ$  coincide). The magnetic field is fixed at  $B \approx 0.0025H_{c2}$  (i.e.,  $a_0/\xi = 50$ ) and the pinning length is  $3\xi$ . The depinning occurs at  $d_{dp} = 0.22a_0$  and the maximal pinning force amounts to  $F_{\text{pin}} = 1.58\epsilon_0$ .

The critical current density  $j_c$  derives from the critical state and, therefore, is related to the maximal pinning force per defect,  $F_{\text{pin}}$ , by [18]

$$j_c = \frac{cnF_{\text{pin}}}{B}. \quad (2)$$

Here,  $n$  is the volume concentration of effective pinning centers which depends on the total defect concentration  $n_0$  and the effective trapping area  $S$  according to  $n = n_0S/S_0$ , where  $S_0 = (\sqrt{3}/2)a_0^2$  is the area of the unit cell. On the basis of the depinning distance  $d_{dp}$  an upper limit for  $S$  is obtained by

$$S = \begin{cases} \pi d_{dp}^2, & \text{if } \pi d_{dp}^2 < S_0, \\ S_0, & \text{otherwise.} \end{cases} \quad (3)$$

Inserting the numerical values  $F_{\text{pin}} = 1.58\varepsilon_0$  and  $d_{dp} = 0.22a_0$  the upper limit for the critical current density becomes

$$j_c \approx 0.4 n_0 a_0^2 \xi j_0, \quad (4)$$

where  $j_0 = (4/3\sqrt{3})(c\varepsilon_0)/(\xi\Phi_0)$  is the depairing current density. Note that  $j_c$  is inversely proportional to  $B$ . For the creep activation energy,  $U(j)$ , we obtain

$$U(j) = U_c \left( \frac{j_c - j}{j_c} \right)^\alpha, \quad (5)$$

with  $U_c = 0.18 \pm 0.02\varepsilon_0 a_0$  and  $\alpha \approx 1.97$ . The exponent  $\alpha \approx 2$ , resulting from the sharp drop in energy at depinning, differs from the value  $5/4$  obtained for a string in a (smooth) washboard pinning potential [19].

Elastic considerations suggest that *extended pinning centers* deform not only the nearest neighboring vortices but also some of the next nearest neighbors and, therefore, all these vortices must be soft. In order to study the effect of extended pins, the magnetic field is fixed at  $B \approx 0.06H_{c2}$  corresponding to  $a_0/\xi = 10$  and the pinning centers are restricted to lengths  $l_p \leq 7a_0$ . Firstly, we analyze the topological aspects of the lattice deformations and, secondly, we determine the critical current density and the activation energy for depinning.

For extended pinning centers the situation is more complicated than for point pins and the lattice deformations produced depend crucially on the angle  $\vartheta$ , the pinning length  $l_p$ , and the distance  $d$ . In order to illustrate the effects of extended pins we consider a pin with a length  $l_p = 3a_0$  dragged along an angle  $\vartheta = 5^\circ$ . At a distance  $d = 0.98a_0$  configurations of four twisted vortices, so-called *twisted quadruplets* (TQ), are formed above and below the pinning center, i.e., a loop and anti-loop excitation of four vortices, see Fig. 2.

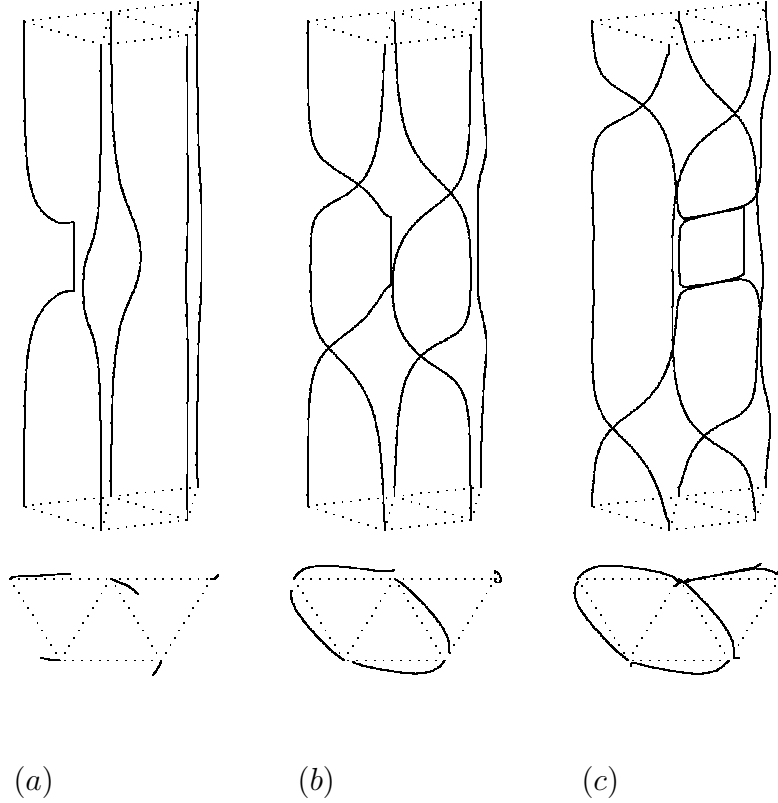


FIG. 2. An extended pinning center with  $l_p = 3a_0$  together with the pinned vortex segment is dragged through the VL at an angle  $\vartheta = 5^\circ$ . Two TQ's appear at  $= 0.98a_0$  and disappear again after the vortex has depinned via a pair annihilation state.

At the transition from the disentangled to the entangled state the deformation energy drops considerably  $\sim (0.5 - 1)\varepsilon_0 a_0$ , see Fig. 3, and becomes slightly larger than the energy of two TQs because the pin is not at a lattice site. The high energy of these loop excitations,  $E_{TQ} - E_0 = 2.41\varepsilon_0 a_0$  ( $E_0$  is the ground state energy of the regular VL), is due to the hexagonal VL which confines the TQ to a length  $l_{TQ} = 2.94a_0$ . The TQs above and below the pinning center have opposite orientation and, therefore, attract each other. The interaction energy of the TQs can be estimated by considering two oppositely oriented vortex rings in parallel planes separated by a distance  $L$ . Choosing vortex rings on top of each other with the same radius  $R$ , we obtain

$$E_L = \pm 2\pi^2 \frac{R^4}{L^3} \varepsilon_0 + O\left(\frac{R^6}{L^5} \varepsilon_0\right). \quad (6)$$

Using the numerically obtained values  $L \approx 6.4a_0$  and  $R \approx a_0$  we find

$$E_L(TQ) \approx -2\pi^2 \varepsilon_0 a_0^4 / L^3 \approx -0.08 \varepsilon_0 a_0. \quad (7)$$

When the pinned vortex segment is at its closest distance from its nearest neighboring vortex, the configuration is similar to the initial state since the TQs “carry away” the displacement of one lattice constant. Therefore, it looks as if the nearest neighbor rather than the original vortex were pinned.

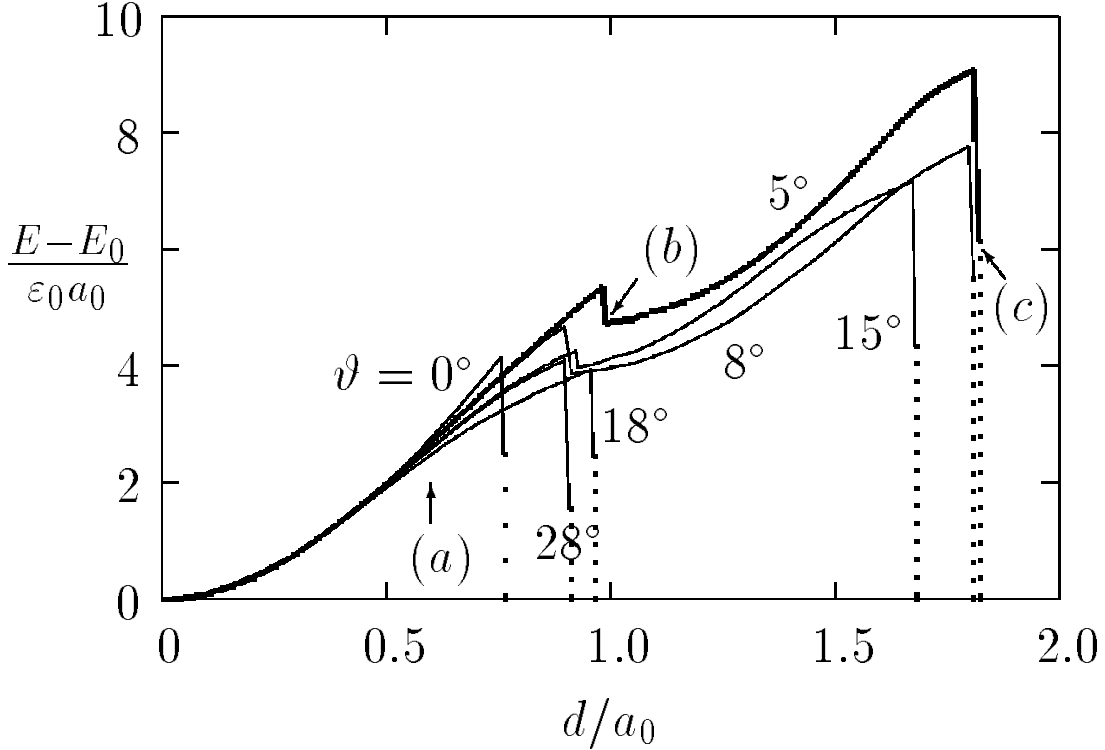


FIG. 3. The deformation energy exhibits a palpable drop when the topology changes, i.e., for a displacement  $d \sim a_0$ . For  $\vartheta = 0^\circ$  a one-loop depinning occurs whereas for small angles, e.g.,  $\vartheta = 5^\circ$ , TQs are generated. Intermediate angles, e.g.,  $\vartheta = 8^\circ$  and  $\vartheta = 15^\circ$  lead to the creation of TTs. For larger angles  $\vartheta = 18^\circ$  and  $\vartheta = 28^\circ$  a pair annihilation state is formed. Note that the largest slope of the energy curve, obtained for  $\vartheta = 0^\circ$ , determines the maximal pinning force and hence the critical current density as well as the orientation of motion. The configurations (a), (b), and (c) are displayed in Fig. 2.

If the pinned vortex segment is dragged beyond the nearest neighboring vortex towards the next nearest neighbor the distance between the TQs is increased. Despite the larger

separation of the TQs, there is not enough space for the creation of a second pair of TQs (this behavior has been obtained for  $l_p \leq 7a_0$ ). Instead, the pinned vortex and the next nearest neighboring vortex form a configuration of two twisted vortices. Since configurations of two twisted vortices are unstable in the VL [17] the two vortices collapse and a *pair annihilation state* is formed, leading to an exchange of the pinned vortex segment, see Fig. 2. After depinning the two oppositely oriented TQs move together and annihilate, leaving behind a “healed” regular VL. The depinning terminates the generation of vortex entanglement associated with the formerly pinned vortex. However, configurations of entangled vortices can be stabilized by other pins, in particular, weak point disorder.

The formation of two TQs is a generic case for extended pinning centers. With increasing angle, the force the pinned vortex exerts onto its closest neighboring vortex is reduced and, therefore, only configurations of three twisted vortices, so-called *twisted triplets* (TT), are generated. The TTs behave similarly to the TQs and, in particular, disappear in the same way. For angles close to  $\pi/6$  a pair annihilation state is formed (note that the twisted pair is unstable in the VL) which in turn leads to an exchange of the pinned vortex segment with the nearest neighboring vortex. The lattice deformations as a function of the angle  $\vartheta$  and the pinning length  $l_p$  are summarized in the “phase diagram” in Fig. 4.

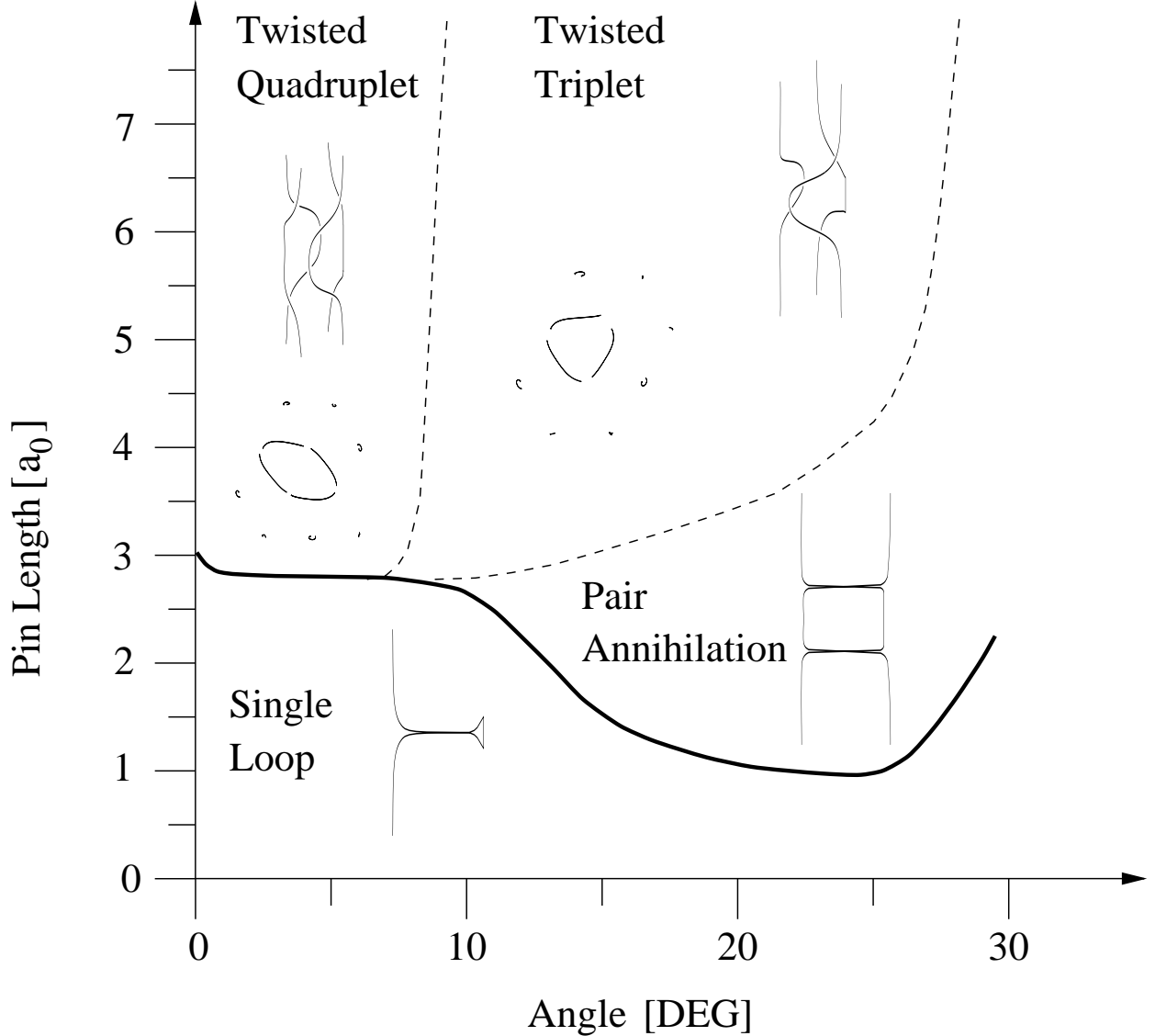


FIG. 4. Extended pinning centers can trigger the formation of configurations with three or four twisted vortices. Below the solid line depinning is mediated by a vortex loop creation at the pin, whereas above this line depinning always involves pair annihilation either with the nearest or the next nearest neighboring vortex.

The strong dependence of the deformation energy on the angle  $\vartheta$ , see Fig. 3, makes the VL move along a lattice vector. This behavior is a consequence of the maximal pinning force which is obtained for  $\vartheta = 0^\circ$ , see Fig. 3. Interestingly, weak pinning seems to introduce the same orientation of motion as has been demonstrated by experiments on Al films [20] as well as by theoretical studies [21,22]. The critical current density for extended pins derives

along the same lines as for point pins, but with  $S = S_0$ , as the change in topology occurs at  $d \sim a_0$ . Accordingly, the critical current density is given by

$$j_c = \frac{3\sqrt{3}}{4} \frac{F_{\text{pin}}}{\varepsilon_0} n_0 a_0^2 \xi j_0. \quad (8)$$

$F_{\text{pin}}$  depends on the field and, therefore, the critical current density is not inversely proportional to  $B$  (as is the case for point pins) but is given by

$$j_c \approx 6.1 \left( \frac{B_{lp}}{B} \right)^\gamma n_0 \xi l_p^2 j_0, \quad (9)$$

with  $\gamma = 0.7 \pm 0.1$ , where  $B = \Phi_0/a_0^2$  is normalized with respect to  $B_{lp} = \Phi_0/l_p^2$ . The activation energy to change the topology, however, exhibits the same scaling behavior as for point-pins

$$U(j) = U_c(l_p) \left( \frac{j_c - j}{j_c} \right)^\alpha, \quad (10)$$

with  $\alpha \approx 2$ ,  $U_c(l_p) = \beta \varepsilon_0 a_0 (l_p/a_0)^\gamma$ ,  $\beta = 1.63 \pm 0.05$  and  $\gamma = 0.78 \pm 0.05$ . The universality of the exponent  $\alpha$  originates from the pronounced edge of the deformation energy when the topology changes.

In conclusion, we have studied the plastic deformations of the vortex lines due to strong pinning. We have identified the relevant depinning processes involving either loop creation or pair-annihilation, depending on the pin size. We have found that large pins do generate entangled configurations (TTs and TQs) which will be stabilized by a finite density of pins. Finally, we have determined the critical current density  $j_c$  as well as the activation barrier  $U(j)$  for creep, the latter showing a universal exponent  $\alpha \approx 2$  originating from the change in topology at depinning.

We gratefully acknowledge the financial support from the Swiss National Science Foundation.

---

[1] M. J. Higgins et al., *Physica C* **257**, 232 (1996).

- [2] A. E. Koshelev et al., Phys. Rev. Lett. **73**, 3580 (1994).
- [3] W. K. Kwok et al., Phys. Rev. Lett. **73**, 2614 (1994).
- [4] A. M. Campbell et al., Adv. Phys. **21**, 199 (1972).
- [5] A.-C. Shi et al., Phys. Rev. Lett. **67**, 1926 (1991).
- [6] A. C. Marley et al., Phys. Rev. Lett. **74**, 3029 (1995).
- [7] A. I. Larkin et al., J. Low. Temp. Phys. **34** (1979).
- [8] A. Brass et al., Phys. Rev. B **39**, 102 (1989).
- [9] F. Nori, Science **271**, 1373 (1996).
- [10] T. Matsuda et al., Science **271**, 1393 (1996).
- [11] K. Harada et al., Nature **360**, 51 (1992).
- [12] S. Bhattacharya et al., Phys. Rev. B **49**, 10005 (1994).
- [13] L. Civale et al., Phys. Rev. Lett. **67**, 648 (1991).
- [14] K. Fossheim et al., Physica C **248**, 195 (1995).
- [15] P. Yang et al., preprint (1996).
- [16] G. Blatter et al., Phys. Rev. Lett. **68**, 875 (1992).
- [17] A. M. Schönberger et al., Phys. Rev. Lett. **75**, 1380 (1995).
- [18] Yu. N. Ovchinnikov et al., Phys. Rev. B **43**, 8024 (1991).
- [19] G. Blatter et al., Rev. Mod. Phys. **66**, 1125 (1994).
- [20] A. T. Fiory, Phys. Rev. Lett. **27**, 501 (1971).
- [21] A. Schmid et al., J. Low. Temp. Phys. **11**, 667 (1973).
- [22] T. Giammarchi et al., Phys. Rev. Lett. **76**, 3408 (1996).